NANJING INSTITUTE OF GEOPHYSICAL PROSPECTING AND INSTITUTE OF PHYSICS PUBLISHING JOURNAL OF GEOPHYSICS AND ENGINEERING

J. Geophys. Eng. **2** (2005) 231–237 doi:10.1088/1742-2132/2/3/007

Seismic tomography using travel-time surfaces for experiments in the laboratory

Cuiping Li and Robert L Nowack

Department of Earth and Atmospheric Sciences, 550 Stadium Mall Drive, Purdue University, West Lafayette, IN 47906, USA

E-mail: cli0713@gmail.com and nowack@purdue.edu

Received 20 May 2005
Accepted for publication 12 July 2005
Published 1 August 2005
Online at stacks.iop.org/JGE/2/231

Abstract

In this paper, seismic tomography using travel-time surfaces was performed for synthetic sediment samples in the laboratory. Travel-time surfaces were used for visualization of the data as well as for quality control. Tomographic experiments were first conducted on numerical test data and then on observed data recorded in the laboratory. For the observed data, the construction of travel-time surfaces allowed for better quality control of the data and identified where travel times needed to be re-picked. It was found that the resulting patterns on the travel-time surfaces were similar between the numerically simulated data and the measured data for similar structures giving added confidence in the travel-time picking procedures. The resulting travel-time tomography inversions were found to be able to reconstruct simple, as well as more complicated, structures in the synthetic sediment samples. But, careful picking of the observed travel times was required based on continuity of the travel-time surfaces to obtain good tomographic results. However, travel-time inversions still result in smoothed solutions and for finer scale features an additional waveform inversion may be required.

Keywords: seismic tomography, inversion, seismic travel times

1. Introduction

Seismic tomography is an important geophysical technique for performing non-destructive testing. In the field, it is often difficult to design a dense tomographic experiment with good angular coverage. However, for samples in the laboratory, it is possible to perform tomographic experiments that are repeatable and have good ray coverage. In this paper, we perform seismic tomography in the laboratory using travel-time surfaces for synthetic sediments with known structures. Travel-time surfaces are used for visualization of the data as well as for quality control. Seismic tomography experiments are set up to measure transmitted seismic waves through the samples from multiple directions. Ray-based travel-time inversion techniques are then applied to the data sets recorded in the laboratory to invert for the structures of the synthetic sediments. The travel-time surfaces are used to identify where travel times need to be re-picked. Lutter *et al* (1990) used reciprocity for quality control of refraction travel times but the construction of travel-time surfaces allows for the comparison of travel times for nearby ray geometries. Travel-time surfaces were also used by Li and Nowack (2004) for autoregressive extrapolation when there is incomplete ray coverage. For this study, travel-time surfaces are used for tomographic inversions of simple, as well as more complicated, structures using a laboratory geometry.

2. Sample preparation and experiment set-up

In our tomography experiments, water-saturated unconsolidated synthetic sediments were created from glass beads saturated with deionized water. The glass beads were manufactured by Potter Industries Inc., and were graded to the maximum roundness and size range with an accuracy of 90% (Li 2002). The glass beads were chosen with an average size of 280 μm. Synthetic water-saturated sediments were then packed in a plastic cylindrical container with a diameter of 220 mm and a height of 300 mm. To improve the homogeneity of the samples, the container was filled with de-ionized water and then the glass beads were slowly poured

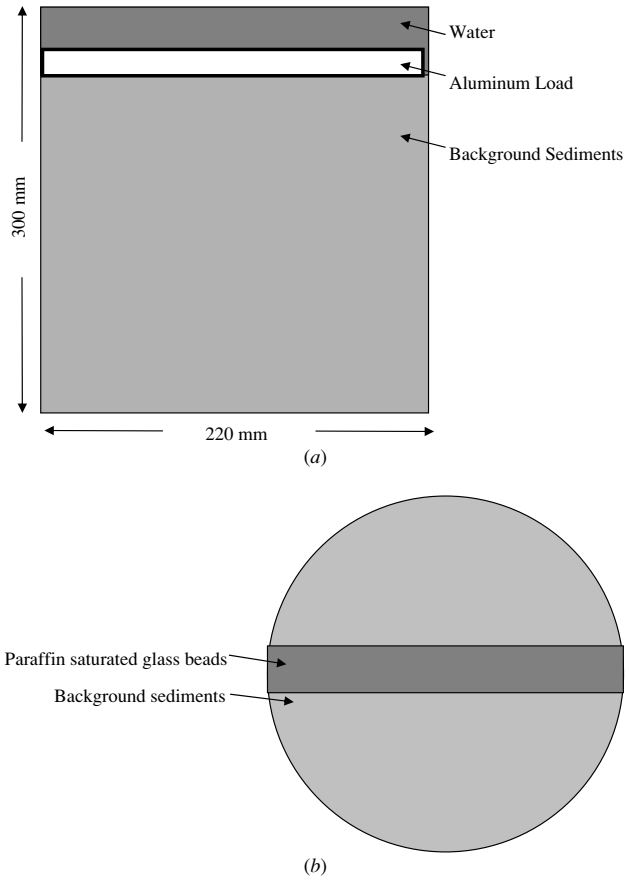

Figure 1. (*a*) Water-saturated background sediments were packed in a cylindrical container with a diameter of 220 mm and a height of 300 mm. An aluminium load was placed on top of the sediments to guarantee the homogeneity of the background sediments. (*b*) An example set-up for the inhomogeneous experiment. A bar made of paraffin-saturated glass beads with a diameter of 280 μm is put into the background sediments.

into the container. When the glass beads were poured, the container was shaken to let the glass beads and water mix with each other more homogeneously. An aluminium load was then placed on the top of the sediment samples to prevent the glass beads floating from the water-saturated background sediments and to ensure the homogeneity of the synthetic sediments (figure 1(*a*)).

Inhomogeneous sediments can be set up in the laboratory to simulate seismic experiments with heterogeneities. Figure 1(*b*) shows one inhomogeneous experimental geometry. For this case, a bar made of paraffin-saturated glass beads with a diameter of 280 μm is put into the background sediments. The bar has a width of about 40 mm, a velocity of about 2.3 km s^{-1} and acts as a high velocity heterogeneity within the background sediment mix.

Seismic tomography experiments were set up to measure the transmitted seismic waves through the synthetic geological media with different internal structures. A sketch of the laboratory set-up is shown in figure 2(*a*). The tomographic imaging system is composed of a high voltage pulse generator (IRCO model M1k-20), an oscilloscope (Lecroy Co. 94136), two computer-controlled rotary stages (Newport Co.

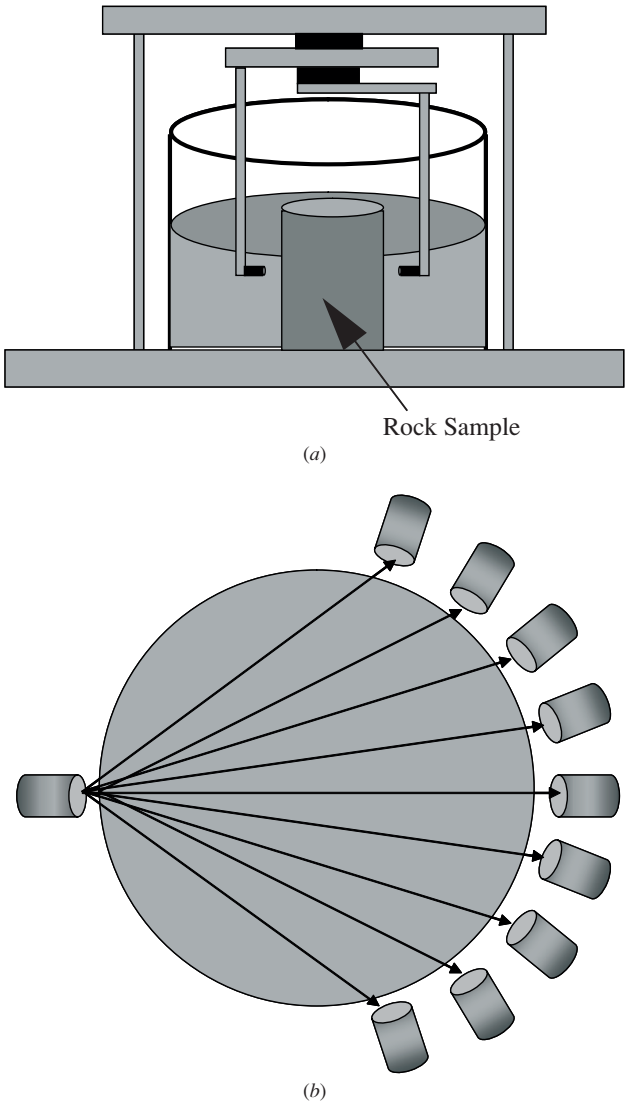

Figure 2. (*a*) Sketch of the experimental set-up. Water-coupled 1 MHz acoustic transducers are used to send and receive the acoustic signals. Two computer-controlled rotary stages are used to move the source and receiver independently. (*b*) Sketch of the source–receiver geometry.

URM100PP and Motion Master 2000) and two water-coupled spherically focused piezoelectric transducers with a central frequency of 1 MHz. One transducer is used as a source to send acoustic signals, and the other is used to receive the acoustic signals after they have passed through the sample. An aluminium holder attaches the source transducer to one of the computer-controlled rotary stages. The rotary stage with the receiver is attached to the second computer-controlled rotary stage. The rotary stage with the receiver is bolted to the rotary stage with the source. As a result, the receiver can rotate with the source and relative to it. Figure 2(*b*) shows an example of the source–receiver geometry.

After the experimental set-up has been aligned according to the alignment procedures and the samples have been prepared and put into the homogeneous background model, acoustic signals are transmitted using water-saturated

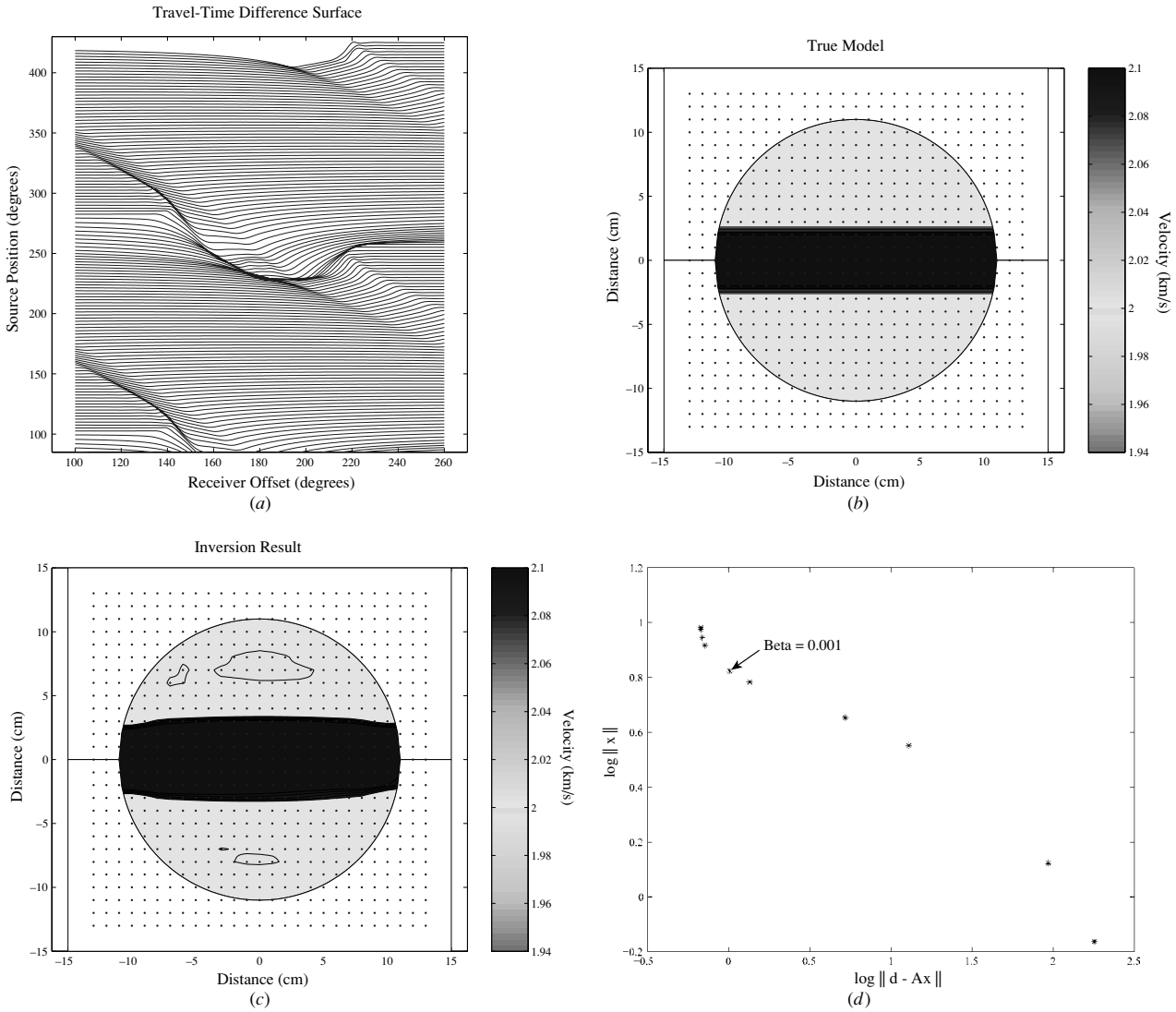

Figure 3. (*a*) Synthetic travel-time difference surface for the true model shown in (*b*). (*b*) The true model with a high velocity bar right across the background model. (*c*) Travel-time inversion result. (*d*) The L-curve was used to select the overall amount of damping to the inversion.

transducers and the travel-time data are collected with an oscilloscope. The source transducer sends out acoustic signals and the receiver transducer receives the waves after they pass through the sample. At each source–receiver location, 15 sweeps of the waves are transmitted and then averaged. The average waveform is then saved to a computer file. In our laboratory tomographic experiments, the transmitted signals are recorded every 2.5° for 67 receiver positions in angular position, resulting in a receiver scan of 165° for each source location. Also, 135 source positions are used with an increment of 2.5°, resulting in a source scan of 335°. This results in a total of 9045 waveforms recorded for each experiment. More details of the experimental procedures can be found in Li (2005).

3. Tomographic experiments on numerical data

A series of numerical simulations with similar internal structures such as the laboratory experiments were performed to test the tomographic reconstruction algorithm. The tomographic inversion applied to the travel-time data to reconstruct the internal sediment structures is described by Li (2005) and uses an approach similar to Wang (1993). In this approach, a variable damping is used to approximately renormalize the problem for unequal ray coverage and variable pixel size. In order to adjust the level of damping, the L-curve approach of Hansen (1998) is used. The amount of damping is determined by the 'knee' of the trade-off curve between the fit to the data and the norm of the model.

Numerical experiments were first conducted to evaluate tomographic response for this source and receiver geometry. The true numerical model for the first experiment consisted of a high velocity bar that spans the diameter of the sample in a background homogeneous model (figure 3(*b*)). This test is used as a reference for experiments on observed data described later. The high velocity bar has a speed of 2.1 km s^{-1} compared to the background sediments of 2.0 km s^{-1}. Rays are traced in the true model using the ray tracing algorithm of Červený *et al*

(1988). A surface plot of the travel-time differences between the true model and the homogeneous background model is given in figure 3(*a*). The travel-time surfaces are shown with respect to source position in degrees and receiver offset from the source in degrees.

A tomographic inversion is applied to the data in figure 3(*a*), and the reconstruction of the synthetic data is shown in figure 3(*c*). The reconstruction in figure 3(*c*) shows a good match with the true model (figure 3(*b*)) except for some broadening. To minimize the broadening effect of the ray theory tomography, an L-curve method was applied to the travel-time data. In this approach, the damping value is chosen at the 'knee' in the trade-off curve between the norm of the model and the fit to the data. According to the L-curve plot shown in figure 3(*d*), we chose 0.001 as the optimal trade-off value. The other synthetic and observed experiments use the same value.

To set up the true model for a second synthetic experiment, the high velocity bar in the first experiment is broken into two pieces and separated in such a way that there is a gap between them. A plot of the true model is presented in figure 4(*b*). Similarly, rays are traced and a surface plot of the travel-time difference surface is presented in figure 4(*a*). The reconstruction using the tomographic inversion has been performed in the same way as in the previous experiment. Figure 4(*c*) shows the inversion result. Comparing the reconstruction (figure 4(*c*)) to the true model (figure 4(*b*)), again, we see a good match where the gap between the two parts of the bar is resolved by the tomographic inversion. The above two synthetic experiments show very good reconstruction results, and greatly improve our confidence in performing the laboratory experiments with similar geometries.

4. Tomographic experiments on observed laboratory data

Using the experimental set-up in figure 2(*a*), two real laboratory experiments with similar geometries to the previous synthetic experiments were performed. To get the travel-time differences, an additional experiment for the homogeneous background model has also been conducted. The travel times were then subtracted between the two experiments to obtain the travel-time difference surface. The transmitted acoustic waves were recorded on computer files, and reconstructions with the picked travel-time differences were then performed.

The true model for the first real data experiment is similar to the one for the first synthetic experiment (figure 3(*b*)). The model is a high velocity bar completely across the background model (figure 5(*c*)). The heterogeneity with a velocity of about 2.3 km s^{-1} is made of paraffin-consolidated glass beads with an average size of 280 μm and the background velocity is about 2.0 km s^{-1}. Figure 5(*a*) shows the initially picked travel-time residuals surface. As can be seen by the travel-time surface there are some rapid changes in travel times that are likely to pick errors since it is unlikely that the adjacent time picks change so rapidly. We use the travel-time surface

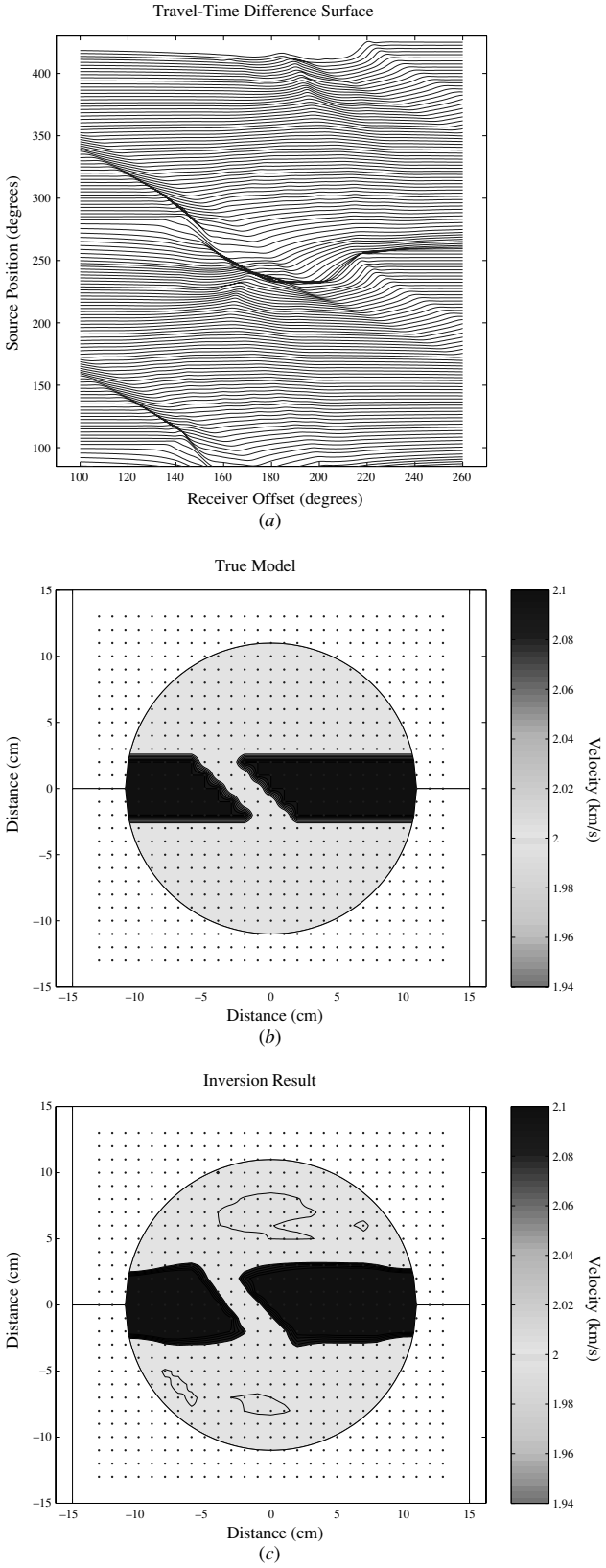

Figure 4. (*a*) Synthetic travel-time difference surface for the true model shown in (*b*). (*b*) The true model with two high velocity pieces arranged in such a way that there is a gap between them. (*c*) Travel-time inversion result.

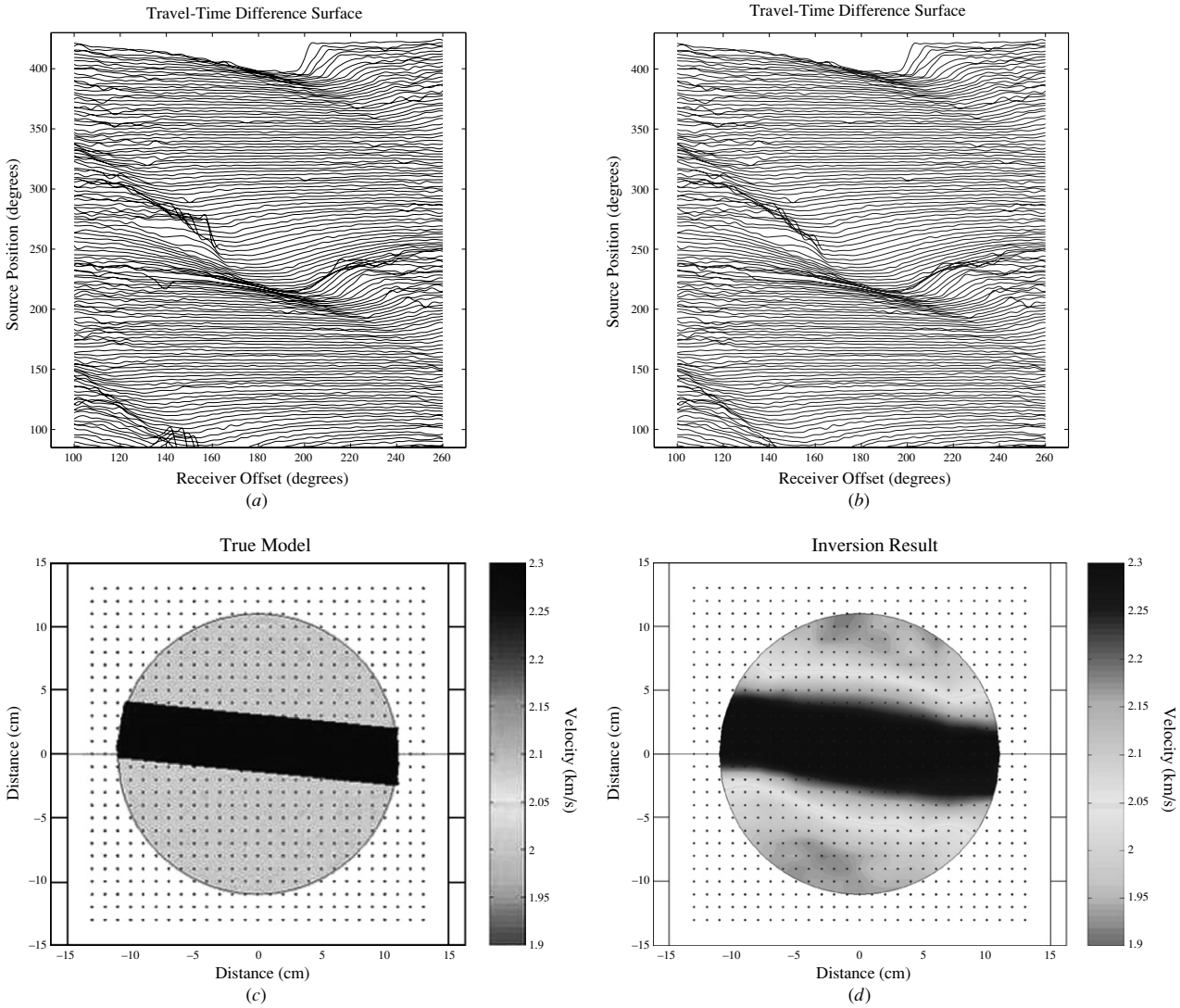

Figure 5. (*a*) Initially picked travel-time difference surface with some picking errors for the true model shown in (*c*). (*b*) Re-picked travel-time difference surface. (*c*) The true model with high velocity bar right across the background model. (*d*) Travel-time inversion result for re-picked data.

plots to identify places where re-picking the travel-time data may be required. The re-picked travel-time surfaces are shown in figure 5(*b*). If we compare figure 5(*b*) to figure 3(*a*), we note that the overall patterns of these two plots are very similar. The comparison of the travel-time surface plots from the synthetic and real experiments gives us further confidence about our travel-time picking.

A tomographic inversion is then performed to do the reconstruction for the experimental data, and the results are shown in figure 5(*d*). The reconstruction shows a good match with the true model although there is broadening at the edges. To minimize the broadening effect of the ray theory tomography, the L-curve analysis has been done to find the optimal value of the trade-off parameter as in the numerical experiments.

The second observed data experiment has a similar geometry as the second synthetic experiment above. Figure 6(*c*) displays the true model for this experiment. The two pieces of high velocity bars are made of the same materials as in the previous experiment, and they have a velocity of about 2.3 km s^{-1}. Figure 6(*a*) shows an initial plot of the picked travel-time difference surface between the true model and background homogeneous model. Again, rapid variations in the travel-time surface are used to identify regions that may require re-picking, and figure 6(*b*) shows the re-picked travel-time surface. Again, the overall patterns of figure 6(*b*) and figure 4(*a*) are similar.

The tomographic inversion result is shown in figure 6(*d*) and there is a reasonably good match with the true model in figure 6(*c*). Although the inversion result is slightly broadened by the smoothing effect of the ray theory tomography, we can still see the gap between the two bars. Overall, the reconstruction with the tomographic inversion in figure 6(*d*) clearly resolves the two bars except for some broadening at the edges. However, for fine-scale features, a waveform or diffraction tomography iteration may be required to obtain

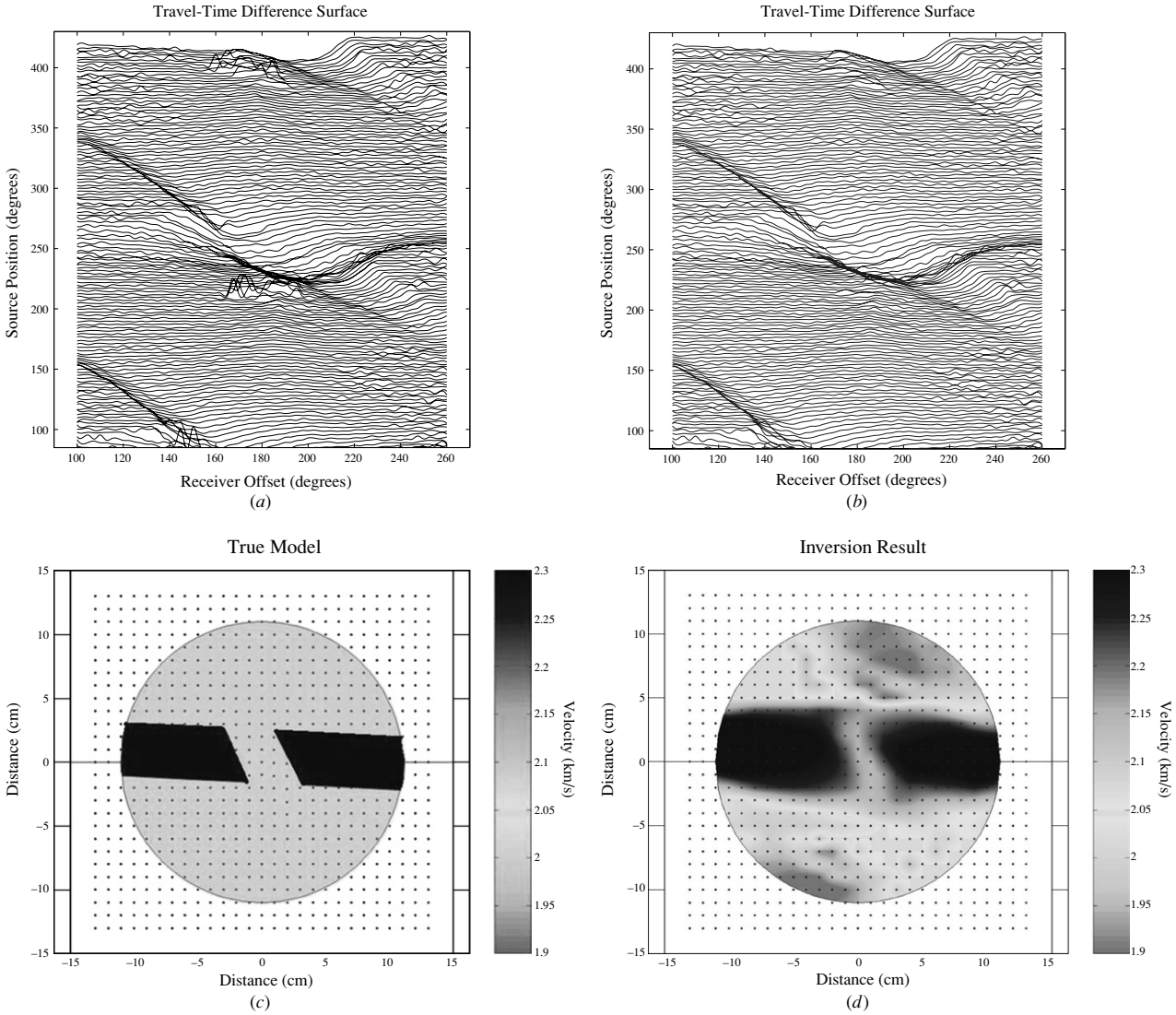

Figure 6. (*a*) Initially picked travel-time difference surface with some picking errors for the true model shown in (*c*). (*b*) Re-picked travel-time difference surface. (*c*) The true model with high velocity bar right across the background model. (*d*) Travel-time inversion result for re-picked data.

better resolution (Lo and Inderwiesen 1994, Pratt 2005, Hole *et al* 2005). The above two real data experiments show that for the laboratory experiments considered travel-time tomography can not only image simple structures, but also can image features of more complicated structures. Also, the plotting of observed travel-time surfaces can be used to evaluate the travel-time picking and identify where re-picking of the travel times is required.

5. Summary

In this study, we have performed seismic tomography using travel-time surfaces for experiments on synthetic sediments with known structures. The travel-time surfaces were used for visualization of the data as well as for quality control of the data. The laboratory experiments were designed to measure transmitted acoustic waves passing through the sediment samples at different angles. To ensure the feasibility of the laboratory experiments, numerical experiments with similar geometries were performed first. The well-resolved structures obtained from the numerical experiments gave us more confidence in performing the real laboratory experiments. As we expected, the travel-time surfaces of the real data obtained from the laboratory experiments showed similar overall patterns with the synthetic travel-time data. Also, plotting the travel-time surfaces allowed for better quality control and identified where travel times needed to be re-picked. The inverted results show that the laboratory tomographic experiments can image both simple structures and more complicated structures. Nonetheless, travel-time inversions still result in some smoothing and an additional waveform inversion may be required for finer scale features.

Acknowledgment

The authors would like to thank Professor Laura Pyrak-Nolte for allowing the first author to use her rock physics laboratory.

References

Červený V, Klimeš L and Pšenčík I 1988 Complete seismic ray tracing in three-dimensional structures *Seismological Algorithms* ed K J Doornbos (San Diego, CA: Academic) pp 89–168

Hansen P C 1998 *Rank-Deficient and Discrete Ill-Posed-Problems: Numerical Aspects of Linear Inversion (SIAM Monographs on Mathematical Modeling* no 4*)* (Philadelphia: SIAM)

Hole J A, Zelt C A and Pratt P G 2005 Advances in controlled-source seismic imaging *EOS Trans. Am. Geophys. Union* **86** 177–81

Li C 2005 Seismic tomography with non-uniform ray coverage and autoregressive extrapolation *PhD Thesis* Purdue University, West Lafayette, IN, USA

Li C and Nowack R L 2004 Application of autoregressive extrapolation to seismic tomography *Bull. Seismol. Soc. Am.* **94** 1456–66

Li X 2002 Tomographic imaging of residual hydrocarbon in water saturated unconsolidated sediments *PhD Thesis* Purdue University, West Lafayette, IN

Lo T W and Inderwiesen P 1994 *Fundamentals of Seismic Tomography (Geophysical Monograph Series* vol 6*)* (Tulsa, OK: Society of Exploration Geophysicists)

Lutter W J, Nowack R L and Braile L W 1990 Seismic imaging of upper crustal structure using travel times from the PASSCAL Ouachita experiment *J. Geophys. Res.* **95** 4621–31

Pratt P G 2005 Velocity models from frequency-domain waveform tomography in controlled source seismology *EOS Trans. Am. Geophys. Union* **86** (18, Abstracts, Spring AGU Meeting, New Orleans) JA372

Wang B 1993 Improvement of seismic travel-time inversion methods and application to observed data *PhD Thesis* Purdue University, West Lafayette, IN, USA